INTERPLANETARY SHOCKS, MAGNETOPAUSE BOUNDARY LAYERS AND DAYSIDE AURORAS: THE IMPORTANCE OF A VERY SMALL MAGNETOSPHERIC REGION

B.T. TSURUTANI[1], X.-Y. ZHOU[1], V.M. VASYLIUNAS[2], G. HAERENDEL[3], J.K. ARBALLO[1] and G.S. LAKHINA[4]

[1]*Jet Propulsion Laboratory, California Institute of Technology, Pasadena, U.S.A.;* [2]*Max Planck Institut für Aeronomie, 3411 Katlenburg, D3411, Lindau, Germany;* [3]*International University of Bremen, P.O. Box 750 561, 28725 Bremen, Germany;* [4]*Indian Institute of Geomagnetism, Colaba, Mumbai/Bombay 400-005, India*

(Received 4 September, 2000; Accepted 2 March, 2001)

Abstract. Dayside near-polar auroral brightenings occur when interplanetary shocks impinge upon the Earth's magnetosphere. The aurora first brightens near local noon and then propagates toward dawn and dusk along the auroral oval. The propagation speed of this wave of auroral light is ~10 km s^{-1} in the ionosphere. This speed is comparable to the solar wind speed along the outer magnetosphere. The fundamental shock-magnetospheric interaction occurs at the magnetopause and its boundary layer. Several physical mechanisms transferring energy from the solar wind directly to the magnetosphere and from the magnetosphere to the ionosphere are reviewed. The same physical processes can occur at other solar system magnetospheres. We use the Haerendel (1994) formulation to estimate the acceleration of energetic electrons to 50 keV in the Jovian magnetosphere/ionosphere. Auroral brightenings by shocks could be used as technique to discover planets in other stellar systems.

Keywords: Aurora, interplanetary shocks, magnetopause

1. Introduction

The magnetopause is defined as a region separating the solar wind plasma and fields from that of the planetary magnetic field region. In the original concept, Chapman and Ferraro (1931) considered the magnetopause to be only a thin current layer. Axford and Hines (1961) introduced the concept of a viscous boundary layer, a broader layer in which momentum and energy are transferred from the solar wind to the magnetosphere. Later Eviatar and Wolf (1968) discussed the possibility of a two-stream instability occurring within the boundary layer, and evaluated the mass diffusion due to wave-particle interactions associated with the instability. See Cowley (1995) for a recent review.

It is now clear that there is a magnetopause boundary layer with a thickness of 1 to 10 proton gyroradii at local noon and ~0.5 R_e at dawn and dusk (Eastman, 1979). Various types of transfer mechanisms have been suggested: magnetic reconnection (Dungey, 1961; Tsurutani and Meng, 1972; Russell and Elphic, 1978;

Surveys in Geophysics **22:** 101–130, 2001.

Gonzalez et al., 1994), direct plasma injection (Lemaire, 1977), and various forms of viscous interaction (Miura, 1995 as one example). Most likely, all of the above mechanisms are operative, but under different interplanetary conditions and with different levels of transfer efficiencies. There is substantial (5–10%) energy transfer through magnetic reconnection during magnetic storms (Gonzalez et al., 1994). The energy transfer through viscous interaction is quit a bit less, ~0.3% (Tsurutani and Gonzalez, 1995).

Several different features characterize the Earth's boundary layer (often called the low latitude boundary layer or LLBL). Ion charge states, velocities, and densities have been used to identify the boundary layer. Figure 1, taken from Eastman and Christon (1995), uses the above ion parameters to not only identify the boundary layers, but to support the idea of mass diffusion across the boundary. He^{++} and the highly charged CNO ion group (all four ions are of solar wind origin) are noted to have decreasing flux with increasing distance from the magnetopause. Energetic He^{+} and O^{+} ions decrease with increasing distance from the inner edge of the boundary layer. These latter ions have their origins in the ionosphere and are energized by ionospheric, magnetospheric and/or plasmasheet processes. This dual particle behavior (decrease of the He^{++} and CNO from the magnetopause inward and decrease of He^{+} and O^{+} outward) has been interpreted as a signature of particle diffusion. Particles diffuse from the magnetosheath into the LLBL, and from the magnetosphere into the LLBL.

Another feature of the LLBL is the presence of broadband electric and magnetic waves (Gurnett et al., 1979; Tsurutani et al., 1998a). These waves have been invoked to scatter the energetic ions (and electrons) across magnetic fields to form part of the LLBL (Tsurutani and Thorne, 1982; Tsurutani and Lakhina, 1997).

There has been a question of what mode these plasma waves are (Rezeau et al., 1989; Treumann et al., 1995; see Lakhina et al., 2000 for a review), and what their origins may be. Figure 2, taken from Anderson et al. (1982), shows the broadband nature of the E and B waves as observed in the ISEE-1 wave spectrum channels. Tsurutani et al. (1998a) showed that 1 min. averages of the magnetic (B) waves had a power-law shape over a frequency range from 3 Hz up to the local electron cyclotron frequency (~500 Hz) and the electric (E) waves a range from 3 Hz to 10^5 Hz (with a power-law shape). In agreement with the original idea of Gurnett et al. (1979), the E and B spectra have been interpreted as broadband whistler mode waves with a superposition of some form of electrostatic emissions.

The purpose of this paper will be to review the most recent results concerning the nature of the boundary layer waves and their sources, and put them into context with aurora physics. A second, related topic is the generation of dayside aurora by interplanetary shock compression of planetary magnetospheres. Possible physical mechanisms for the aurora will be discussed. Finally, some predictions of shock-auroras at the outer planets (and also for astrophysics) will be made.

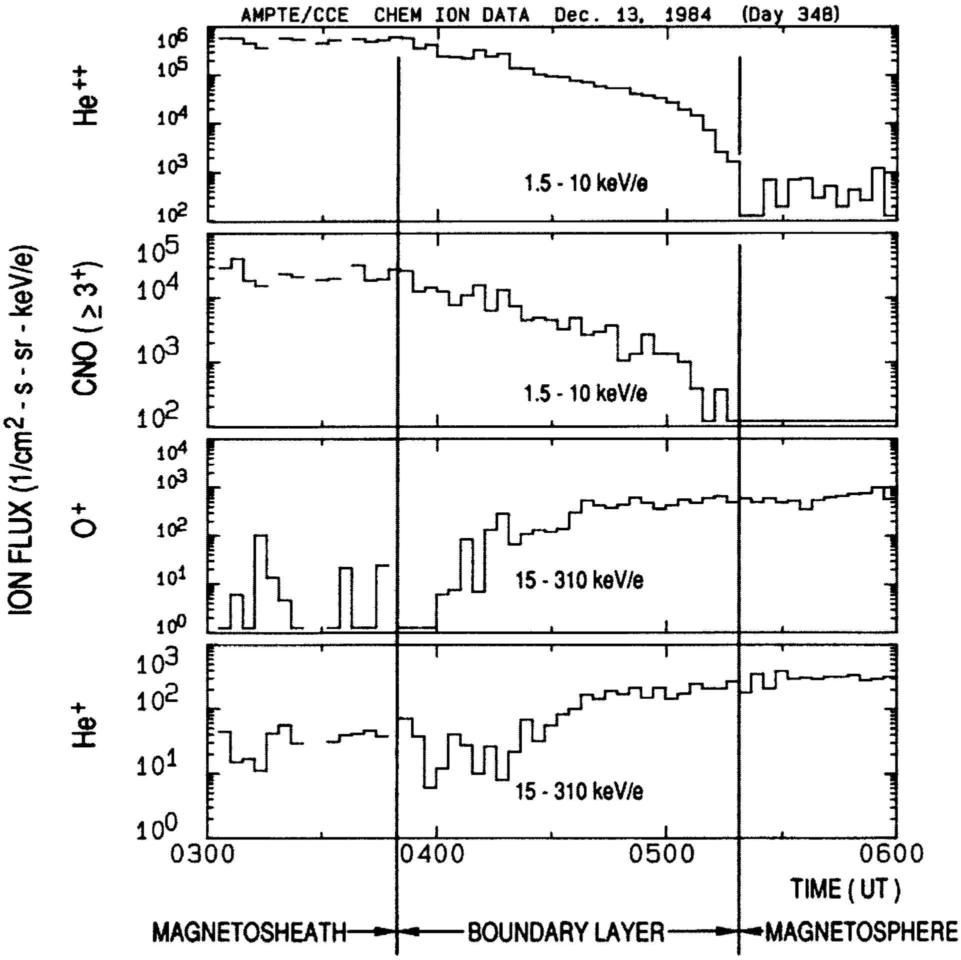

Figure 1. The magnetopause boundary layer. The boundary layer is defined as a region just inside the magnetopause where there is a mixture of solar wind origin and magnetospheric origin of energetic ions.

2. POLAR: Polar Cap Boundary Layer (PCBL) Waves

The NASA POLAR spacecraft orbit near the start of the mission is shown in Figure 3. The POLAR perigee is $\sim$1.8 R_e and apogee $\sim$8 R_e. POLAR does not cross the LLBL but does cross magnetic field lines that map into this region. A recent study (Tsurutani et al., 1998a) has shown that similar broadband E and B waves are detected at POLAR orbits ($\sim$96% of the time), independent of the interplanetary magnetic field north-south direction (i.e., independent of whether magnetic reconnection is occurring or not). In this same study, it was noted that nightside waves were found near apogee and were similar in nature to those discussed earlier by Gurnett and Frank (1977) from Hawkeye 1 and IMP 6 satellite studies. Because

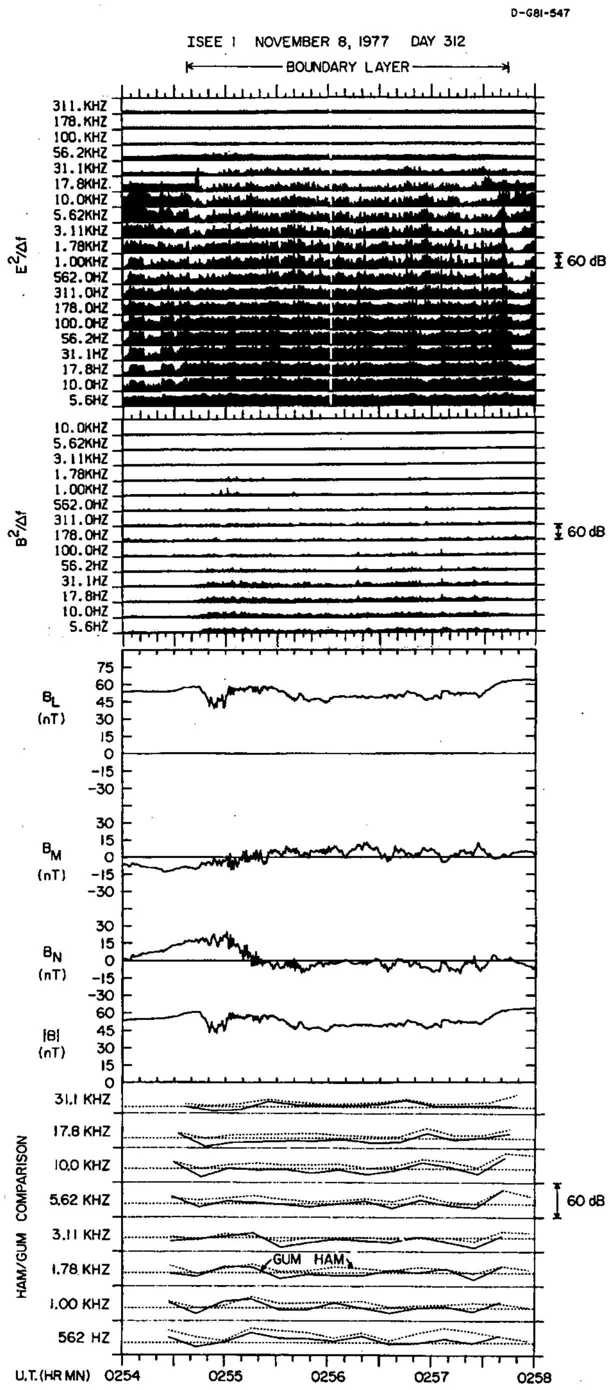

Figure 2. Broadband plasma waves in the boundary layer. Taken from Anderson et al. (1982).

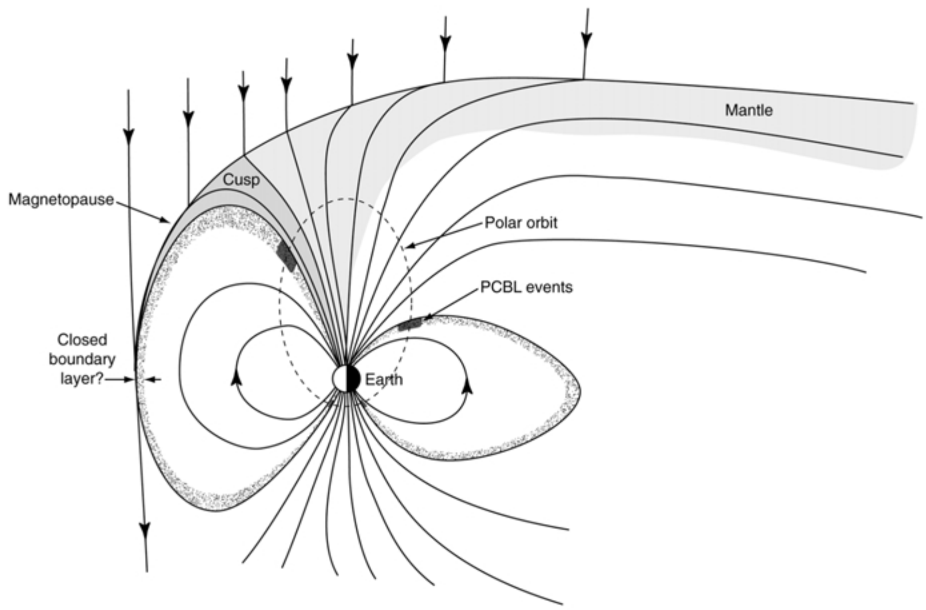

Figure 3. The POLAR spacecraft orbit and regions of detection of PCBL plasma waves.

the waves were detected on magnetic field lines bounding the polar cap, they were named Polar Cap Boundary Layer (PCBL) waves.

The most recent results concerning the PCBL waves are found in Tsurutani et al. (2001a). One year of POLAR PCBL wave occurrences were identified in the SFR data summary plots, and the MCA 14 frequency channels of B waves and 20 channels of E waves were averaged over these intervals. The wave events of the two apogee intervals and two perigee intervals were identified, and the time intervals recorded. The latitude versus local time distribution is shown in Figure 4. The near-apogee data is indicated by the positive latitude data and the near-perigee data by the negative latitude data, corresponding to the POLAR orbit previously shown in Figure 3. The waves are detected 96% of the time for near-apogee passes. The near-apogee waves are detected at $\sim$75° at local noon and $\sim$65° at local midnight. The waves are detected 100% of the time for the near-perigee passes. The latitude location of the near-perigee waves is similar (but with greater spread) to that of the near-apogee waves.

The northern and southern hemisphere PCBL wave locations map out 'ovals'. These 'ovals' are essentially identical to the Feldstein auroral ovals identified by optical and magnetic ionospheric activity measured from the ground. The latter is displayed as Figure 5, and is taken from Feldstein and Starkov (1970) for 'moderate' geomagnetic activity levels.

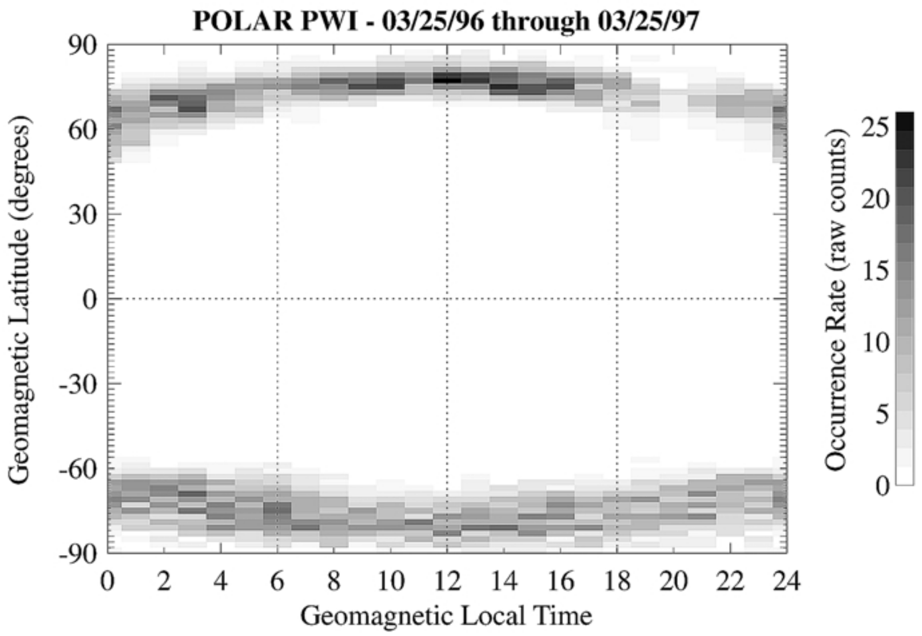

Figure 4. The PCBL plasma wave latitude – local time distributions. The waves map out the northern and southern auroral zones.

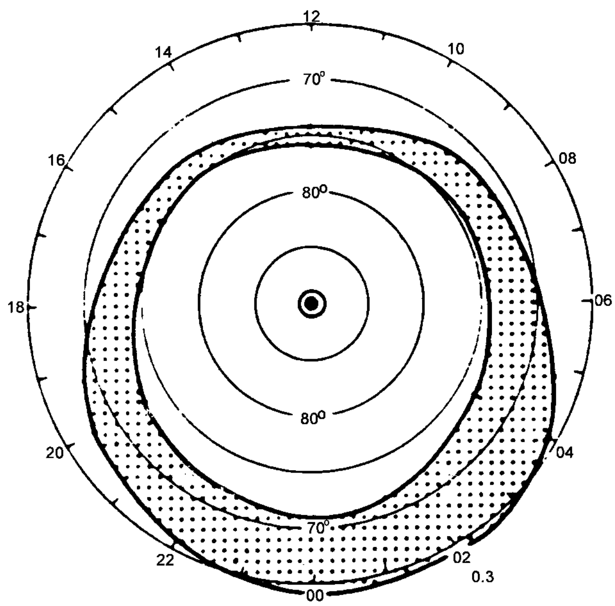

Figure 5. The Feldstein 'auroral oval'. The wave PCBL locations shown in Figure 4 are essentially the same as the auroral oval.

The nature of the PCBL waves has been identified using the POLAR wideband information. High time resolution wave examples are shown in Figures 6 and 7, taken from Tsurutani et al. (1998b, 2001a). Both figures show the wave E and B components in a coordinate system aligned relative to the local ambient magnetic field direction. Both parallel and perpendicular components (to the magnetic field) are shown. In Figure 6, $\sim$10 ms bursts of whistler wave packets are clearly present in the magnetic channels. These emissions occurred at a frequency of $\sim$4.9 kHz during an interval when the local electron cyclotron frequency was $\sim$5.5 kHz. Assuming that the waves are generated locally by a cyclotron resonant interaction with an electron beam, the parallel electron kinetic energy would be $\sim$100 eV. This is the approximate energy of auroral electrons.

Another feature that can be noted in Figure 6 is how fast the wave characteristics/modes can change. By 0827:17.19 UT, $\sim$50 ms later, strong parallel electric component waves dominate. This rapid change in the wave character is typical of the wideband wave data analyzed.

Figure 7 shows parallel electric bipolar pulses (the electric field polarization is along the ambient magnetic field direction) in the dusk sector. These pulses are almost purely electric, but it has been noted that sometimes, there is an associated magnetic component as well (Tsurutani et al., 1998b). It has been speculated that the magnetic component is detectable by the search coil sensors when the bipolar pulses are temporally very broad. Thus a magnetic component may always be present during bipolar pulses, but for rapid bursts, the high frequency magnetic intensities may be below the sensitivities of standard search coil sensors (search coil sensitivities are strongly frequency dependent). Aircore loops would be superior for future diagnoses. The electric bipolar pulses are similar but lower in intensity than those detected at lower altitudes by the S3-3 (Temerin et al., 1982), Viking (Koskinen et al., 1987; Bostrom et al., 1988) and FAST (Carlson et al., 1998; Ergun et al., 1998a, b) spacecraft. Such bipolar pulses have been interpreted as being electron holes (Muschietti, et al., 1999; Goldman et al., 1999a, b), generated by a two-stream instability (Omura et al., 1994; 1999; Goldman et al., 1996b). The above and other discrete plasma wave modes (such as electric waves at the electron plasma frequency) have been detected at a variety of local times. To date, only six intervals at four local times (noon, dusk, midnight and dawn) have been examined in detail in the wideband data. Due to the vast amount of data, a more complete search has not been possible to date.

Figure 8 is a MCA survey plot of the waves for a dusk (17.6 LT) interval. The most intense wave interval (in red) occurs at $\sim$1330 UT at a L shell of 6.7, a distance of 4.9 R_e and a dipole latitude of 31.8°. This example is a relatively simple wave event. More complex events have been detected.

Figure 9 is the corresponding d.c. magnetic field onboard POLAR. The data is shown in GSM coordinates where $\hat{x}$ is radially towards the sun, $\hat{y} = (\hat{\Omega} \times \hat{x})/|\hat{\Omega} \times \hat{x}|$ where $\hat{\Omega}$ is the south magnetic pole of the Earth, and $\hat{z}$ completes the right-hand system. Note that the waves are detected at locations where the sharpest gradients

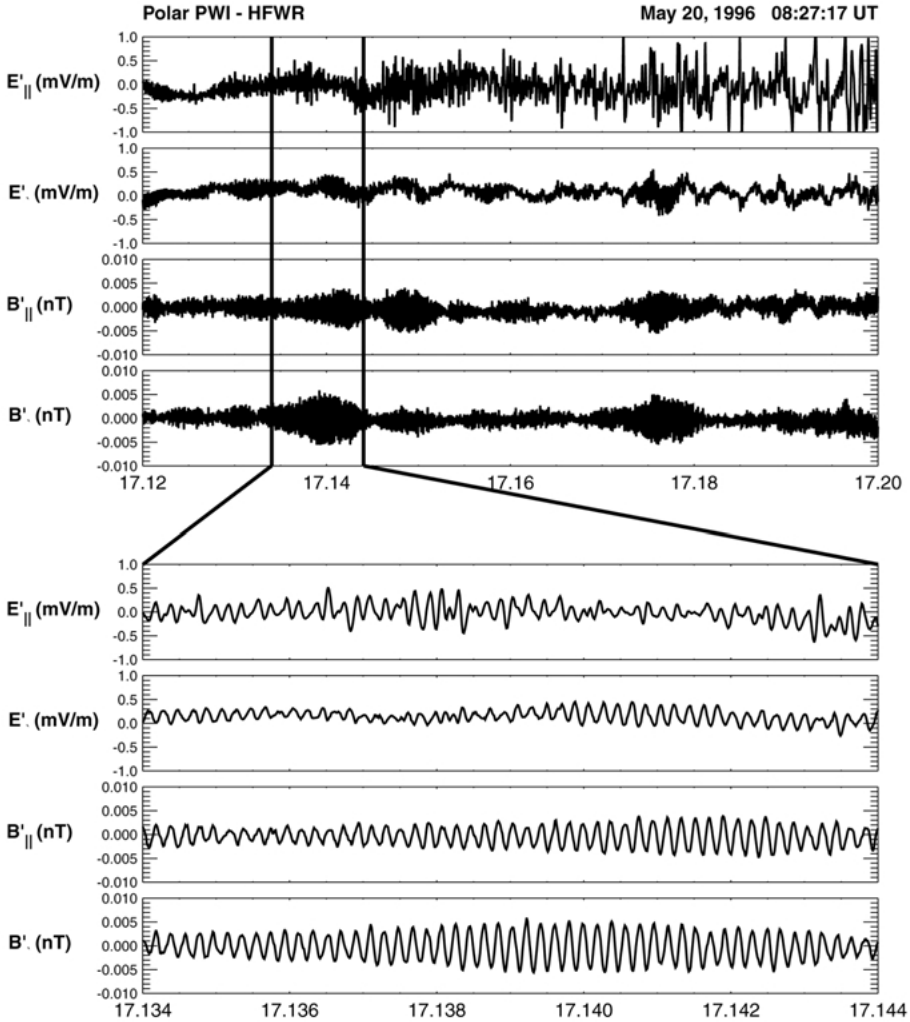

Figure 6. A high-time resolution snapshot of the PCBL plasma waves.

in the magnetic field are present. The field gradients indicate the presence of field-aligned currents (Elphic et al., 1998). Other examples have been studied and the strong correspondence between the presence of intense waves and magnetic field gradients has been noted.

3. Fast Results

Figure 10, taken from Elphic et al. (1998), contains field and particle data from the FAST satellite (see Carlson et al., 1998 for an overview). The satellite was crossing

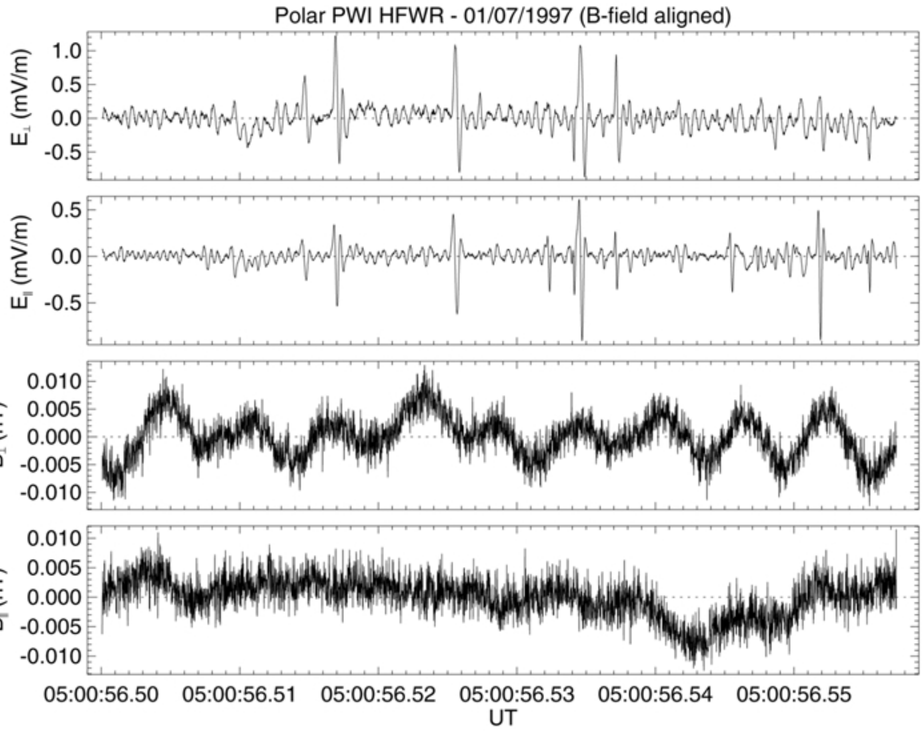

Figure 7. Electric bipolar pulses present in the boundary layer at POLAR near-apogee altitudes.

the near-midnight auroral zone (21.9 MLT) on February 1, 1997. These data are taken from normal auroral arcs. The top panel gives the eastward perturbation fields indicating the field-aligned currents associated with the measured electron beams and the electron fluxes. The bottom three panels show the local potential, electron energy and pitch angle distributions. The shaded vertical regions denote upward beams of electrons carrying strong downward currents. In the middle region between 26:10 and 27:10 UT is a region where there are mono-energetic (∼1 keV) electrons directed downward towards the Earth (last panel).

Figure 11, also taken from Elphic et al. (1998), is an interpretation for observations like those found in Figure 10. Downward currents are indicated by dark downward pointed arrows, with upward currents in-between (upward pointed shaded arrows). These currents are carried by ∼keV electrons. The currents in the ionosphere connecting the upward and downward currents are indicated, as well as the ionospheric electric fields. The FAST orbit occurs at altitudes above these ionospheric regions, and POLAR, at much, much higher altitudes still.

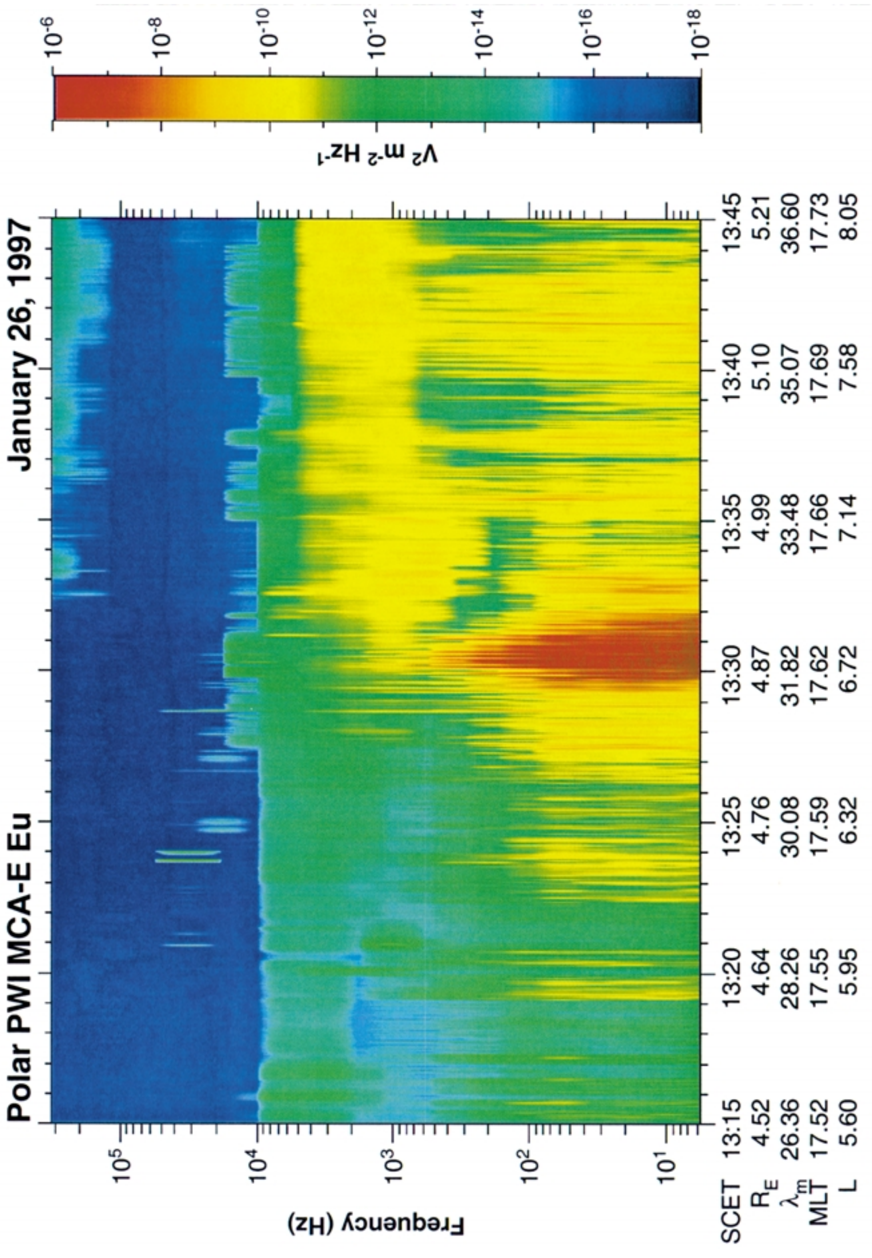

Figure 8. A MCA survey plot of the waves during a dusk crossing of the boundary layer.

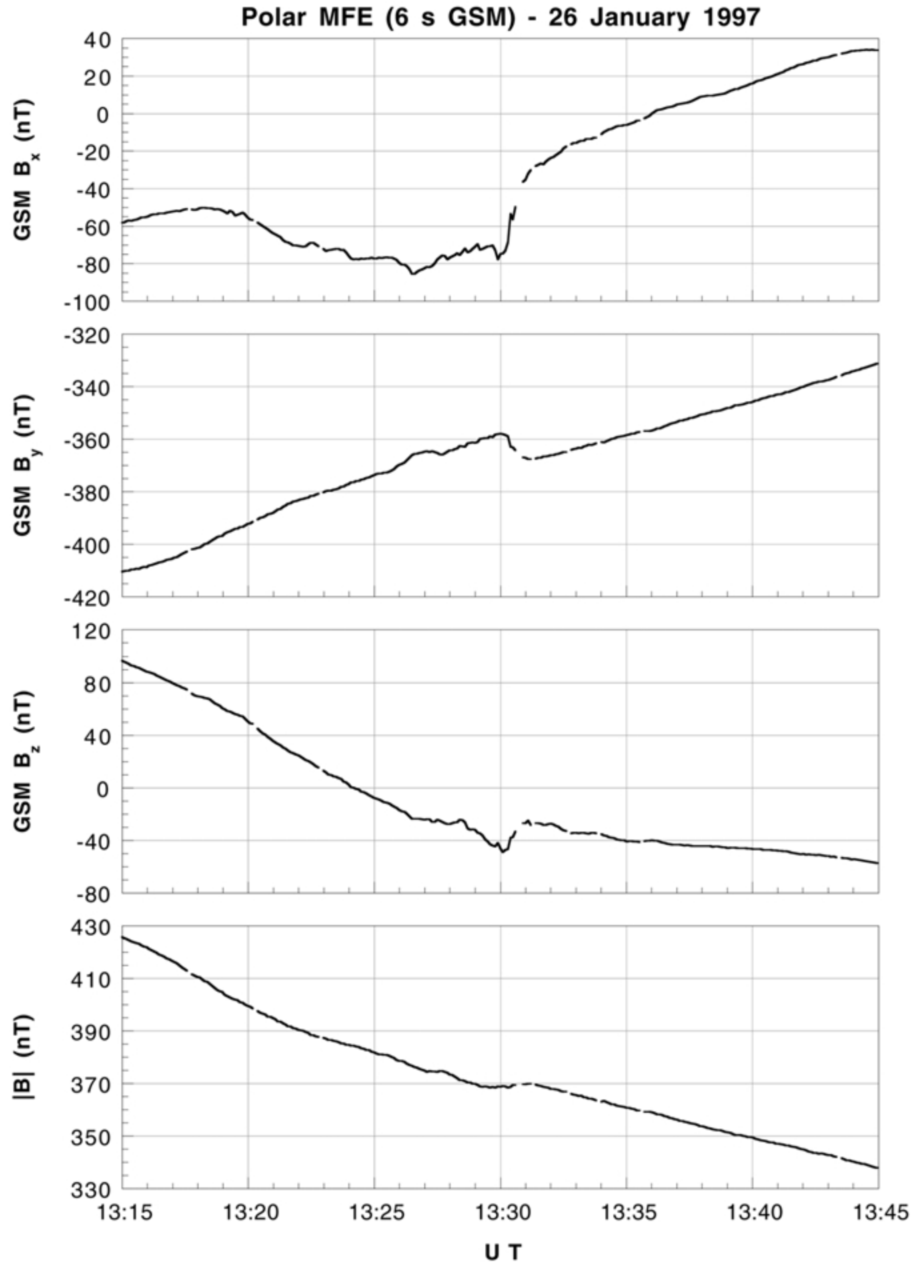

Figure 9. The magnetic fields for the same time interval as in Figure 8. The waves are present where there are strong field-aligned currents.

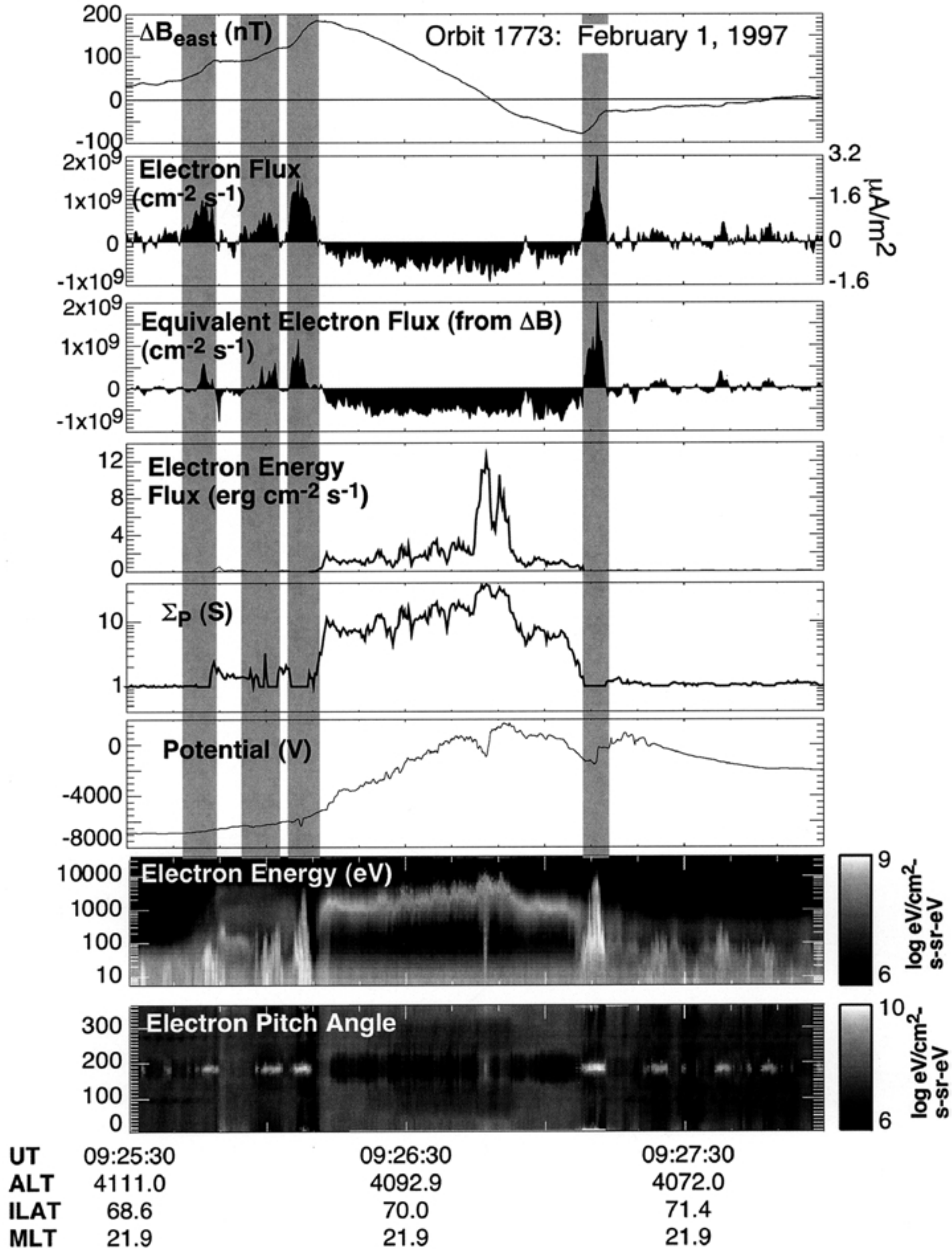

Figure 10. Auroral zone low altitude fields and particle data taken by FAST instruments. Taken from Elphic et al. (1998).

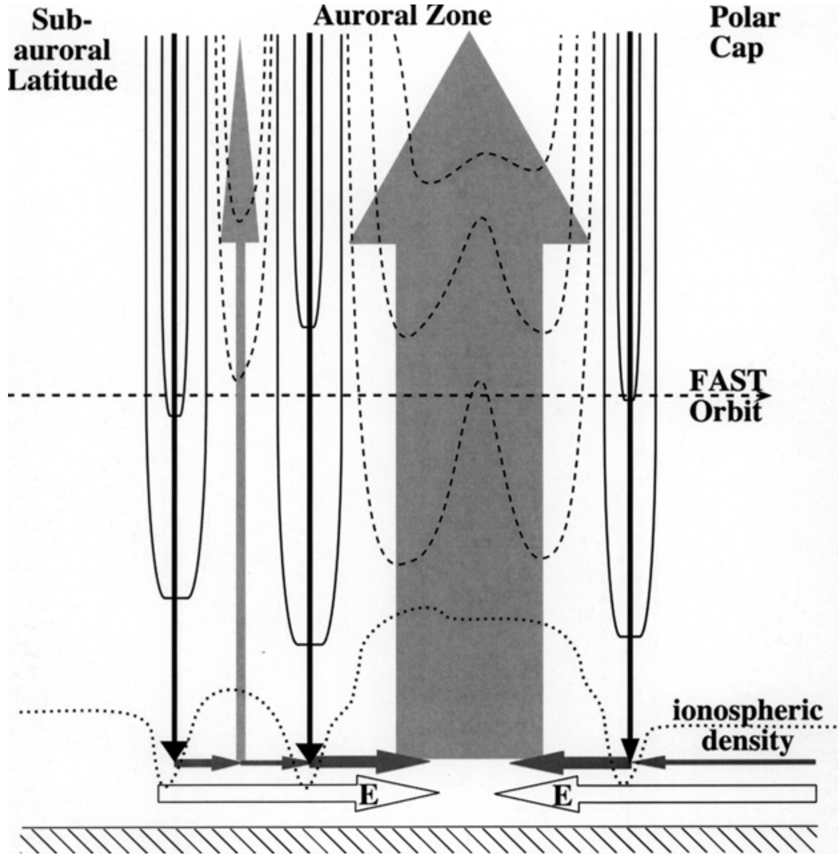

Figure 11. An interpretation of auroral zone currents and precipitating and upflowing particles. Taken from Elphic et al. (1998).

4. Current Understanding of the PCBL/LLBL/Auroral E and B Plasma Waves

Summarizing the above, it now appears obvious that the LLBL, PCBL and auroral zone waves are on the same general magnetic field lines, auroral zone field lines (however, it should be noted that there could be substantial differences in the waves at different altitudes, local times and levels of geomagnetic activity). The POLAR magnetic waves are electromagnetic whistler mode waves which are propagating at frequencies between the proton cyclotron frequency (∼2 Hz for POLAR near-apogee field strengths) and the electron cyclotron frequency (∼5 kHz). These whistler mode waves are bursty and occur at different frequencies (due to different energy electron beams), giving a broad power-law electromagnetic spectrum when averaged over 10 min. or even 10 s (see Anderson et al., 1982 for a discussion of LLBL wave burstiness). The whistler bursts presumably form most of the low frequency electric power law spectrum as well.

There are also (nearly) pure 'electric' signals present within the PCBL. The bipolar pulses are often present at POLAR with large amplitudes ($\sim$1 mV/m), primarily at noon and midnight, but at all local times. As mentioned previously, these do have a small magnetic component as well. There are also parallel electrostatic oscillations somewhat below the electron plasma frequency as well as oscillations at the electron plasma frequency. These discrete electric emissions contain 'power' at the high frequency end of the spectrum, and presumably represent the electric power at frequencies above the electron cyclotron frequency. Thus the initial hypothesis of Gurnett et al. (1979) that the broadband waves are a superposition of electromagnetic whistler mode and 'electrostatic' waves can be supported.

Matsumoto et al. (1994) discovered that the broadband electric noise (BEN) detected in the plasmasheet boundary layer was not at all broadband, but instead composed of discrete bipolar pulses in the time-domain (discussed previously). This GEOTAIL finding led space plasma scientists to rethink ideas about 'broadband' plasma waves everywhere. The GEOTAIL results strongly influenced the thinking and direction concerning POLAR plasma wave studies. Furthermore, our present results indicate that BEN may also not be purely 'electrostatic' as well.

The PCBL waves are found to be most intense in strong field- aligned current regions at POLAR near-apogee altitudes. This observation argues for the strong possibility that the waves are either channeled by depleted (or enhanced) plasma density tubes or are locally generated by field-aligned currents. Lakhina and Tsurutani (1999a, b) have argued for the latter, and these new observations support this. Clearly as the electron beams propagate away from the ionosphere, adiabatic decompression will maintain the beam until the particle 'free energy' is exhausted. Whether particle beams or wave plasma density channels, or both, are present or not at POLAR altitudes is still not known. However, the ISEE-1 results (Anderson et al., 1978; Parks et al., 1979; Tsurutani et al., 1981) indicate that field-aligned electron and ion beams are present within the LLBL. Preliminary POLAR particle measurements indicate that the same is true at POLAR altitudes. With the much improved POLAR instrumentation and the upcoming Cluster II instrumentation, these issues of local generation of the waves should be soon resolved.

Our present view of the LLBL has now been strongly revised by the POLAR and FAST results, even though neither spacecraft directly crosses into the LLBL. There is magnetosheath plasma diffusion or injection into the boundary layer field regions, but far more is happening there than previously thought. Our present scenario is that the solar wind interaction with the magnetosphere leads to cross-polar cap potentials, which in turn lead to field-aligned potential drops and the acceleration of particle beams. These particle beams lead to the waves which enhance the boundary layer cross-field diffusion (in the near-equatorial plane).

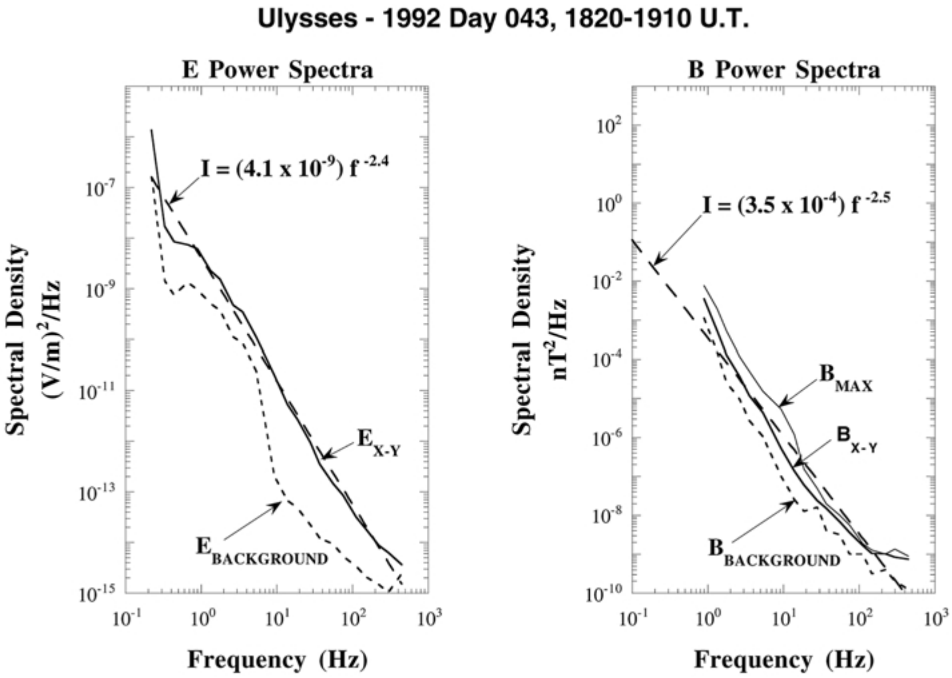

Figure 12. Jovian boundary layer plasma wave spectra. The spectral shape and cutoff (at the electron cyclotron frequency) of the magnetic waves is the same as for boundary layer waves at Earth. Taken from Tsurutani et al. (1997).

5. Jovian Boundary Layer Waves

The Jovian magnetosphere also has a plasma and plasma wave boundary layer inside its magnetopause. The plasma boundary layer was originally detected during the Pioneer 10 and 11 encounters (Intriligator and Wolfe, 1976; Reiff and Hill, 1979) and more recently by Ulysses (Phillips et al., 1993). Model calculations of the MP and BL thicknesses and field orientations were made by Sonnerup et al. (1981). Measurements of the Jovian LLBL waves was performed using Ulysses magnetometer and plasma wave results (Tsurutani et al., 1993, 1997). It is the properties of the latter phenomenon that we will now review here.

Figure 12 shows the electric (left panel) and magnetic (right panel) wave spectra integrated over the LLBL pass (50 min interval). Unfortunately, wideband (high time resolution) wave data are not available on the Ulysses URAP (Stone et al., 1992) plasma wave instrument. Although the wave intensities are relatively weak, waves are clearly present and have a power law shape. Table I summarizes the Jovian LLBL electric and magnetic wave spectral shapes (bottom line), and also those previously measured at Earth.

It is noted that the Jovian wave E and B spectra shapes are nearly identical to those measured at Earth. The magnetic wave intensities are highest at low frequen-

TABLE I

Summary of boundary layer plasma wave observations at Earth and Jupiter.

Spacecraft	Location	Date	B' $(nT)^2/Hz$	E' $(V/m)^2/Hz$
ISEE 1	Earth's magnetopause	day 314, 1977	$\sim f^{-3.3}$	$\sim f^{-2.2}$
Gurnett et al. (1979)				
ISEE 1, 2	Earth's magnetopause	1977	$(1.0 \times 10^{1})\ f^{-3.9}$	$(3.0 \times 10^{-5})\ f^{-2.8}$
Tsurutani et al. (1981)				
ISEE 1, 2	Earth's magnetopause	1977	$(7.90 \times 10^{-2})\ f^{-2.9}$	$(6.3 \times 10^{-6})\ f^{-2.2}$
Anderson et al. (1982)				
GEOS 2	Earth's magnetopause	day 240, 1978	$(3.60 \times 10^{1})\ f^{-2.6}$	$(1.20 \times 10^{-6})\ f^{-2.6}$
Rezeau et al. (1989)				
ISEE 1	Earth's magnetopause	1977–1978	$(3.00 \times 10^{-1})\ f^{-3.3}$	$(6.0 \times 10^{-7})\ f^{-2.1}$
Tsurutani et al. (1989)				
POLAR	~7–8 R_e altitude	day 098, 1996	$(1.17 \times 10^{-2})\ f^{-2.6}$	$(1.19 \times 10^{-7})\ f^{-1.8}$
Tsurutani et al. (1998)	~2 R_e altitude	day 103, 1996	$(1.34 \times 10^{-2})\ f^{-2.5}$	$(1.22 \times 10^{-6})\ f^{-1.8}$
ULYSSES	Jupiter's magnetosphere	day 043, 1992	$(2.0 \times 10^{-4})\ f^{-2.4}$	$(4.0 \times 10^{-9})\ f^{-2.4}$
Tsurutani et al. (1995)				

cies decreases with increasing frequency. The wave power cuts off at the electron cyclotron frequency. The electric spectrum continues on to higher frequencies. Thus, Tsurutani et al. (1997) have concluded that the Jovian BL waves are again most likely an admixture of electromagnetic whistler mode waves plus electric waves. A reasonable assumption is that similar to the Earth's case, bipolar pulses and electron plasma oscillations are present within the Jovian BL and contribute to the high-frequency ($f > f_{ce}$) portion of the electric spectra.

6. Interplanetary Shocks and Dayside Auroras

It has recently been shown that interplanetary shocks cause propagating dayside auroras (Zhou and Tsurutani, 1999; Tsurutani et al., 2001b). Presumably, shocks are directly transferring energy from the interplanetary medium to the boundary layer fields and plasma. The strong particle precipitation into the ionosphere is a consequence of the energization. Figure 13 shows an interplanetary shock (dashed vertical line) detected at WIND at ~0053 UT January 10, 1997. At the time, WIND was 85 R_e upstream of the Earth. The shock is noted by the abrupt magnetic field magnitude, plasma velocity, density, and ram pressure increases across its structure.

The shock velocity has been calculated and its arrival time at the dayside magnetopause predicted. Figure 14 shows the northern auroral zone prior to and after the calculated shock arrival time. In each image, noon 60° latitude is at the top, and the magnetic north pole at the center. Time increases from the top-left image, across to the right and then down. In the top-left image, prior to shock arrival, there is faint dayside aurora present from 03 LT through noon to 15 LT. In the next image, at 0103:48 UT, there is a sudden brightening between 10 to 12 LT at ~75° latitude. The shock was calculated to arrive at ~0103 UT to ($X = 10\ R_e$) just shortly before the image was taken. Thus, there is excellent agreement between the calculated shock arrival time and the local noon auroral brightening. Zhou and Tsurutani (1999) studied 18 interplanetary shock-auroral events in 1997–1998 and found that the calculated arrival times were in agreement to within ~1 min for every case.

In subsequent images, the auroral brightening moves towards local dusk and also towards local dawn. The latter propagation direction is opposite to the direction of gradient and curvature drift of energetic electrons, the usual direction of motion of the aurora during geomagnetic activity (substorms).

Table II shows the ionospheric propagation speeds of the aurora for three shock-aurora events. The speeds are only approximate values, as the 'motion' was derived from images separated in time (as was illustrated in Figure 14). These speeds are found to be ~6 to 11 km s^{-1}, much higher than 'typical' auroral speeds of 1–2 km s^{-1} during substorms (Akasofu, 1977). Assuming the auroras occur on L $\approx$ 10 magnetic field lines, mapping dipole magnetic fields to the equatorial plane will give antisunward velocities of 280 to 370 km s^{-1}. The observed magnetosheath or

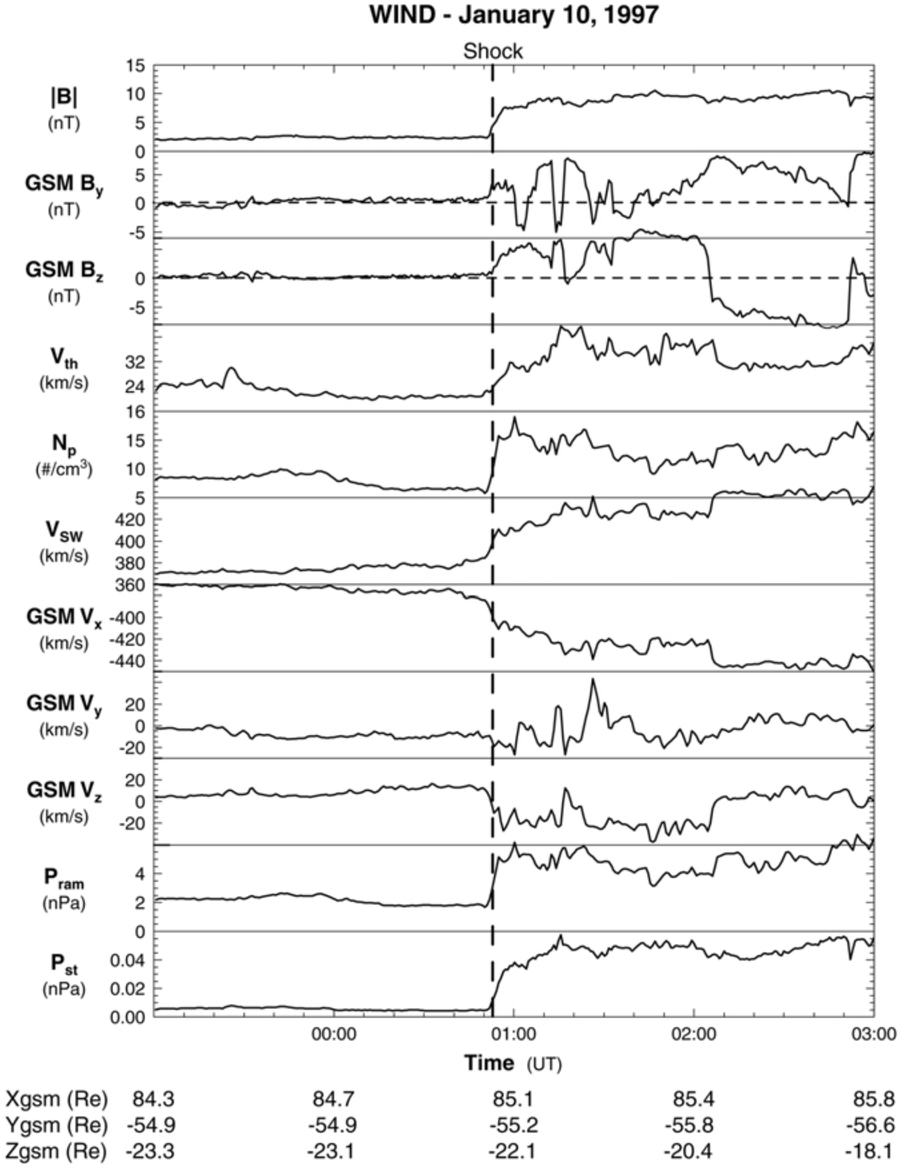

Figure 13. An interplanetary shock detected by WIND. This shock cause a dayside aurora at Earth.

solar wind flow speeds (indicated in the Table) are comparable to the latter values. Zhou and Tsurutani (1999) and Tsurutani et al. (2001b) thus concluded that shock compression of the magnetosphere was responsible for direct energy transfer from the solar wind to the magnetosphere, and that this transfer propagated as a front in the downtail direction at the interplanetary shock speeds.

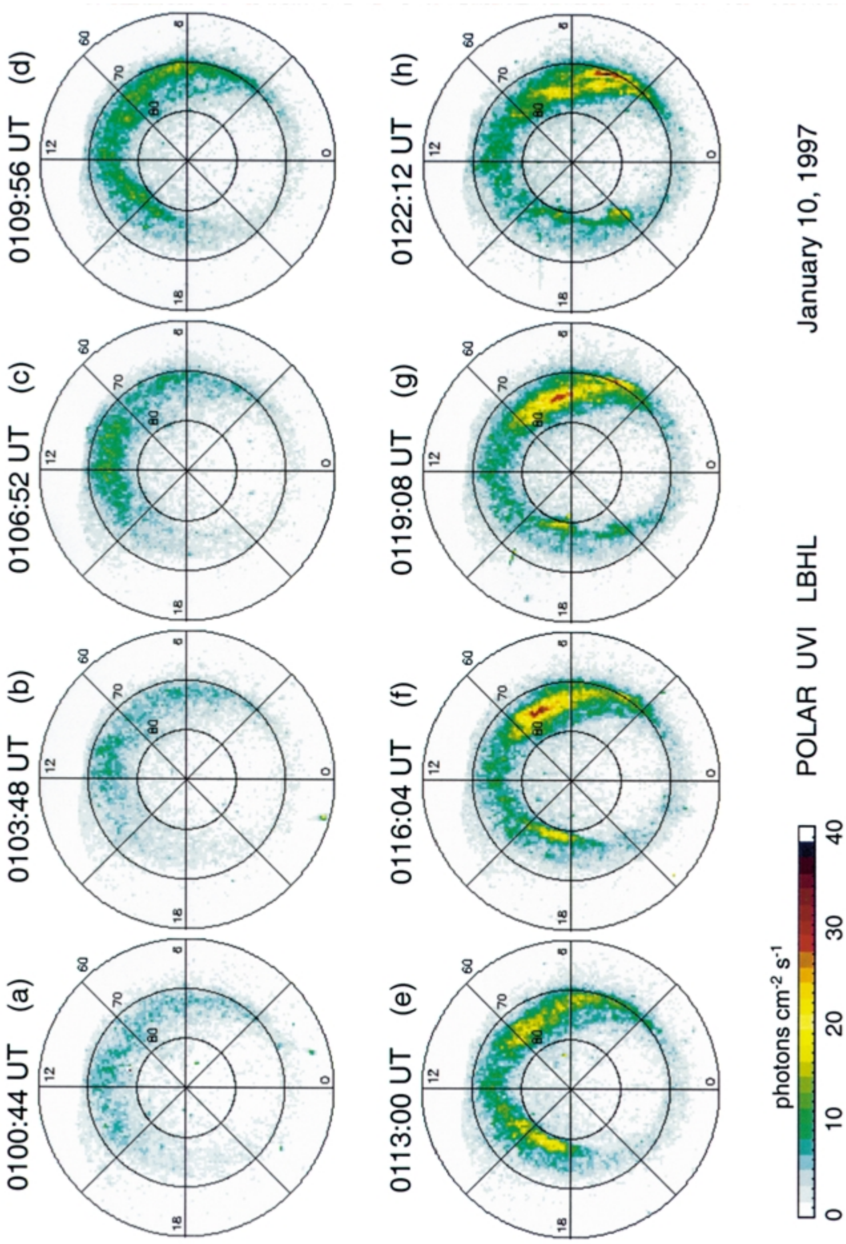

Figure 14. The dayside aurora caused by the interplanetary shock impingement on the magnetosphere.

TABLE II

Auroral ‘speeds’ in the ionosphere (derived from successive Polar UVI images), speeds mapped into the magnetosphere, and comparative solar wind velocities.

Event	Ionospheric V (km/s)	Mapped V* (km/s)	Observed $V_{sh/sw}$ (km/s)	Spacecraft position (R_e)	
10 Jan 1997	6 (dusk)	280	300	I-T (Sheath)	(−19, 19, 10)
1 Oct 1997	10 (dusk)	370	460	IMP-8 (SW)	(10, 32, −3)
10 Dec 1997	11 (dawn)	365	360	GT (SW)	(−4, −25, −0.5)

*Assuming a dipole field of L = 10.

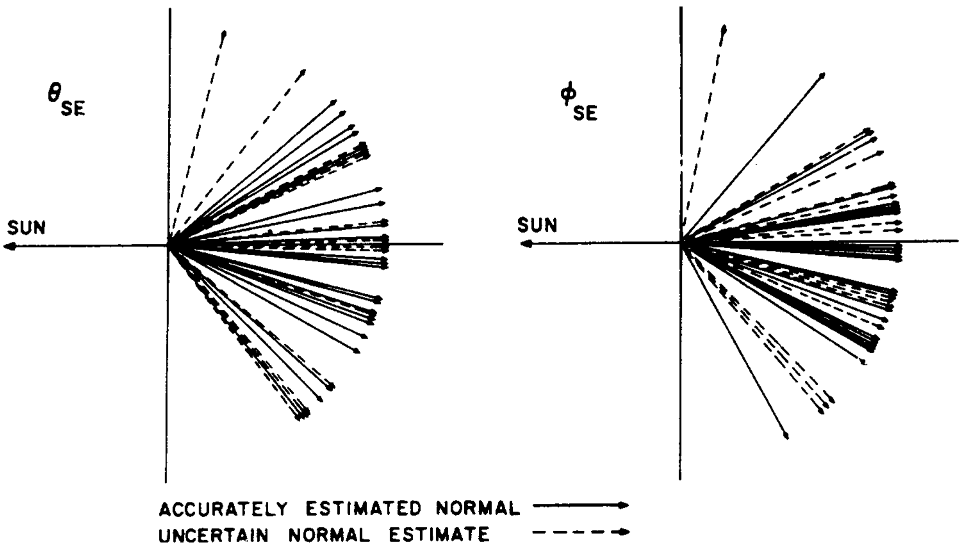

Figure 15. Interplanetary shock normal angles. Taken from Chao and Lepping (1974).

It should also be noted that interplanetary shock waves do not always have their normals along the Sun-Earth line. Although the ‘fast’ solar ejecta come out from the sun more-or-less radially, the shocks formed in the antisolar direction have finite, nonplanar surfaces, and it is this latter property that can lead to significant nonradial shock orientations at 1 AU.

A very nice display of the variability of interplanetary shock normal angles at 1 AU is shown as Figure 15, taken from Chao and Lepping (1974). The shock normals were determined by assuming magnetic coplanarity. There is considerable deviation from radial ($\hat{x}$), both in latitude (θ_{SE}) and azimuth (φ_{SE}) angles.

For the 18 shocking auroras studied by Zhou and Tsurutani (1999), there was a good relationship between the shock orientation and the initial location of the dayside auroral brightenings. One example of an auroral response to an ‘oblique’

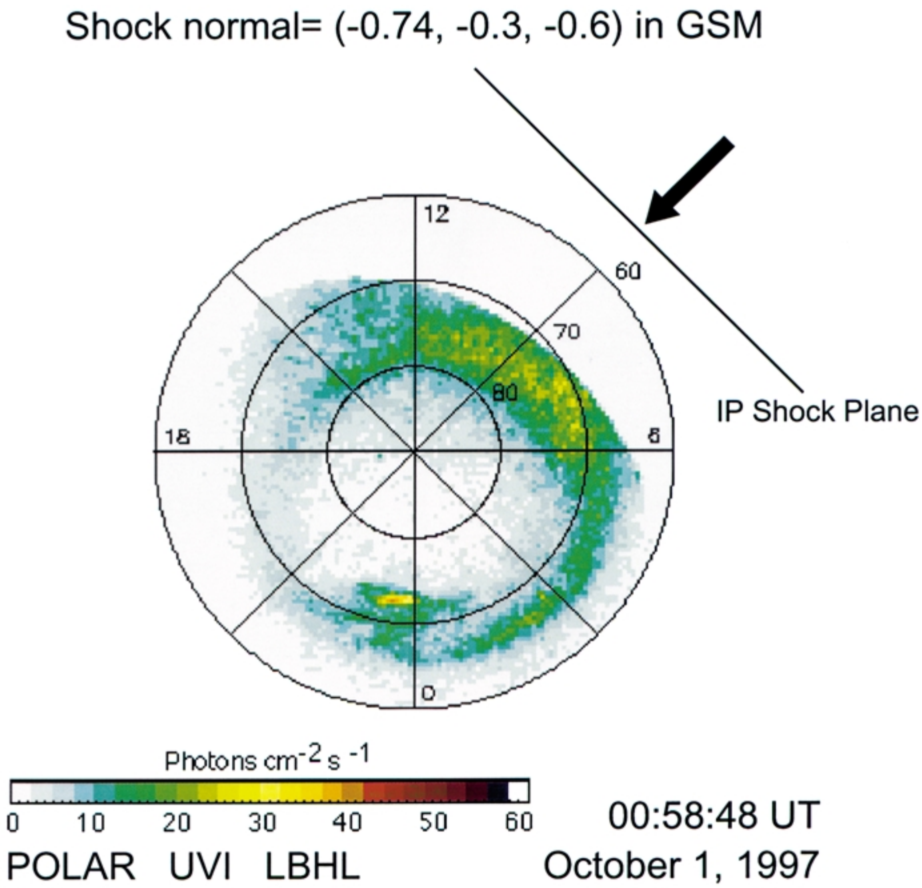

Figure 16. An example of an oblique shock impingement on the magnetosphere and auroral brightening at ~900 local time.

shock event is shown in Figure 16. The shock normal direction was calculated. The shock plane is estimated to hit the magnetopause at a local time of ~0900. The UV image indicates that brightening initially occurs there.

7. Shock-Aurora Mechanisms

7.1. Adiabatic compression

To explain the Earth's shock-auroras, two possible physical mechanisms have been proposed. At this time, it is unclear which mechanism is the dominant one. In the left panel of Figure 17, we show the compression/instability mechanism proposed by Zhou and Tsurutani (1999). The right panel is a schematic of the compression/parallel electric field mechanism proposed in Tsurutani et al., (2001b). The

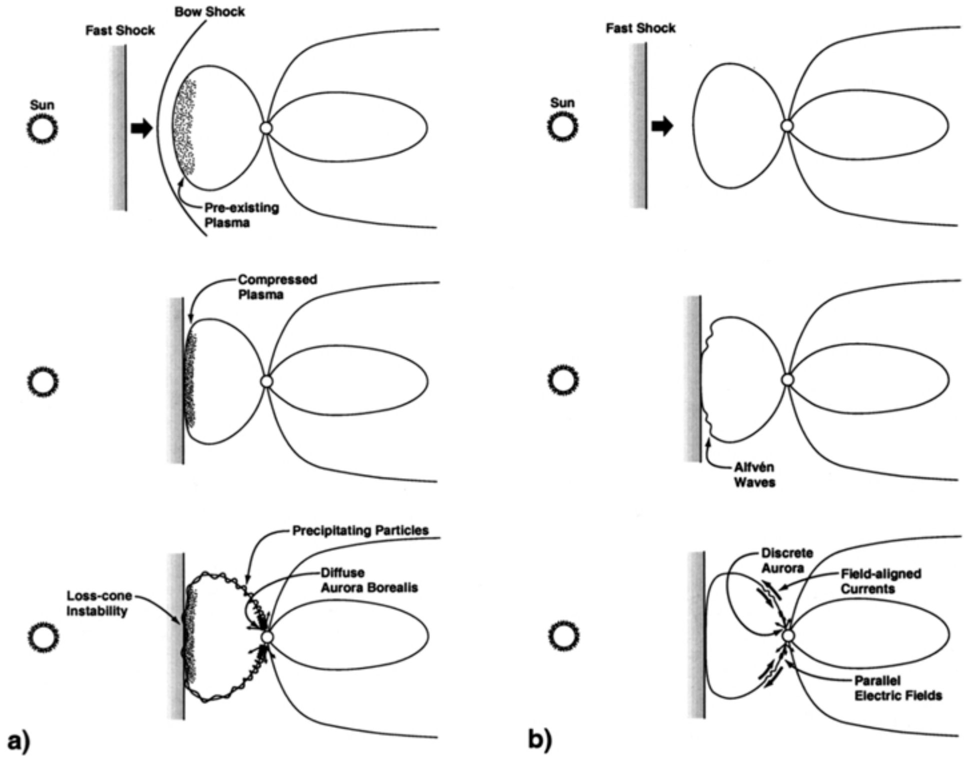

Figure 17. Two possible mechanisms for explaining auroras produced by interplanetary shock impingement.

former mechanism leads to diffuse aurora while the latter will lead to discrete auroral arc formation.

In the compression/instability (left panel) mechanism, the shock ram pressure causes not only compression of the earth's dayside magnetic fields, but also the plasma contained therein. By the conservation of the first adiabatic invariant, the plasma will be heated primarily in the perpendicular (to the magnetic field) direction, leading to strong temperature ($T_\perp/T_\parallel > 1$) anisotropies. Electron (and proton) loss cone instabilities will result, leading to plasma wave growth and particle losses into the auroral zone (and lower L shell) ionosphere due to pitch angle diffusion.

This mechanism consists of conversion of solar wind kinetic energy into magnetospheric dayside electron and ion heating. Since the magnetospheric electrons have much higher velocities, one would expect predominantly electron aurora to result, similar to nighttime substorm auroras. The type of aurora would be 'diffuse' in nature.

7.2. Jovian auroras

Jupiter's aurora taken by the Hubble Space Telescope UV Camera (courtesy of J. Clarke), is shown in Figure 18. Note that there are two northern auroral ovals, a fainter oval poleward of the brighter, lower latitude oval. The bright oval can have intensities of 200–300 kR and the poleward oval is generally fainter, ~100 kR. The Jovian aurora and its dynamics have been reported by Prangé et al. (1993, 1997) and Clark et al. (1998). Prangé et al. (1997) have noted that the scale size of the auroral arcs are similar in size to the Jovian boundary layer mapped into the ionosphere, 230 ± 100 km. Because of the strong and highly variable ring currents within the Jovian magnetosphere, determining whether the magnetopause boundary layer maps into the higher latitude ring or not, is highly uncertain at this time. The more intense lower latitude ring has been found to be (slightly) poleward of the footprint of the satellite Ganymede, so this auroral oval is relatively low in magnetic latitude.

The compressibility of the Jovian magnetosphere by an interplanetary shock is schematically shown in Figure 19. The left-hand panel indicates why the compression factor at Jupiter is much higher than that at the Earth. The Jovian magnetosphere is highly inflated due to the presence of an intense ring current/current sheet. The diamagnetic effect of these particles weakens the local fields and extends the magnetosphere outward into interplanetary space. Shock compression will increase both the particle perpendicular kinetic energy (described previously) and the magnetic field gradient. Both effects will lead to rapid gradient drift of the outer zone energetic ions out of the dayside magnetosphere, allowing a rapid collapse of the magnetosphere.

The loss of Jovian boundary layer energetic particles by the filling of the loss cone (via wave-particle interactions) has already been examined by Tsurutani et al. (1997). Using measured Ulysses particle fluxes, the energy deposition was calculated assuming rapid pitch angle scattering (strong diffusion). It was found that the maximum loss rate by this process was orders of magnitude too low to account for the known auroral brightnesses. Thus for the case of interplanetary shock compressions of the Jovian magnetosphere, it is most likely that the adiabatic compression mechanism may not be able to cause significant auroras. Thus some other type of mechanism should be sought.

7.3. Field-aligned potential drops

The compression/parallel electric field mechanism (right-hand panel of Figure 17) will create enhanced field-aligned currents. When the particle fluxes within the loss cone are too small to provide the necessary currents, field-aligned potentials effectively create much larger loss cones to supply the necessary currents (Carlson et al., 1998; Carlson personal communication, 2000). We will apply the model of Haerendel (1994) here to estimate the parallel electric fields applied to shocks impinging on the Jovian magnetosphere.

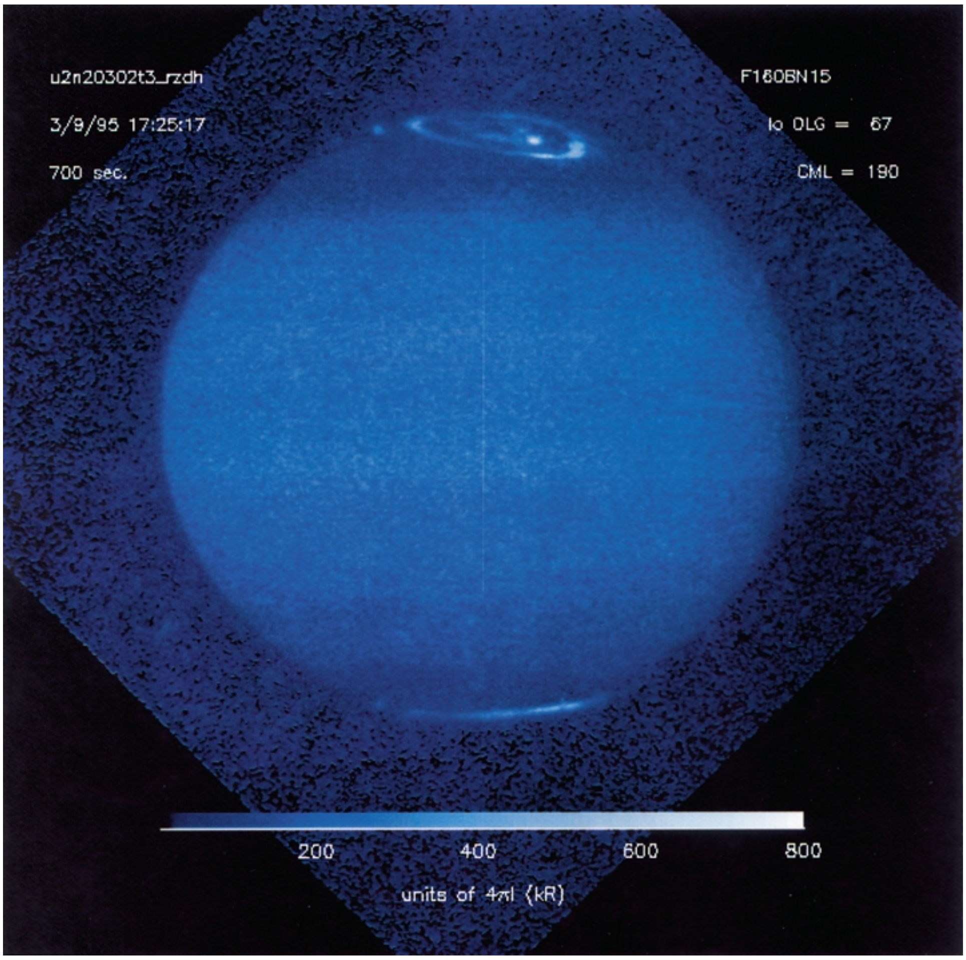

Figure 18. Jovian auroral bands taken by the Hubble Space Telescope. The image is courtesy of J. Clarke.

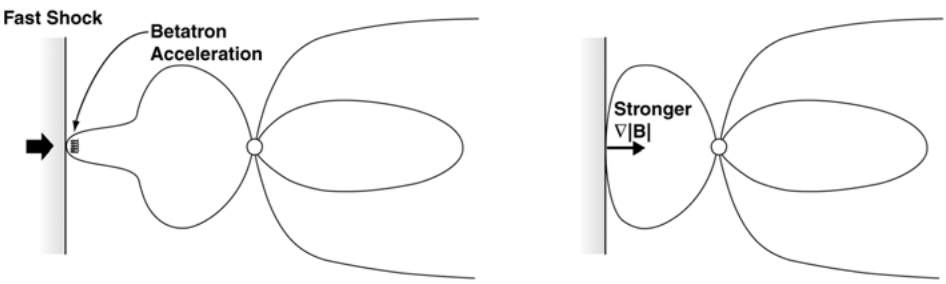

Figure 19. The compressibility of the Jovian magnetosphere by an interplanetary shock.

The order of magnitude auroral field-aligned potential drops can be calculated by making some simple approximations. The field- aligned current can be estimated using Ohm's law:

$$j_{\parallel} = k\phi_{\parallel} \quad (1)$$

where k^{-1} is the mirror impedance equal to $m_e C_{BL}/e$ and n_{BL} (Lyons, 1980), where m_e, C_{BL}, e and n_{BL} are the electron mass, Alfvén speed, the electron charge and plasma density in the boundary layer. Following Haerendel (1994), we can assume field-aligned current focusing from the equatorial boundary layer to the ionosphere is given by:

$$j_{\parallel} = J_{\parallel BL} B_C / B_{BL}. \quad (2)$$

Here $j_{\parallel BL}$, B_C, B_{BL} are the parallel current in the BL, and the field magnitudes of the ionosphere and boundary layer, respectively. We use the measured values of the boundary layer: $B_{BL} = 5$ nT, $n_{BL} = 0.1$ cm^{-3} and the Sonnerup et al. (1981) determination of the width of the BL (~7000 km). A potential of ~50 kV is derived, assuming that the perturbation field (~5 nT) is essentially the same as the ambient field.

It is interesting to note that this potential (~50 kV) is comparable to what Jovian physicists now believe electron energies must be to create the Jovian aurora (Grodent et al., 2000). This has been inferred in order to produce a H_2-FUV emission peaking at 245 km. In support of this general concept, highly field-aligned beams of electrons and ions have been detected during the Ulysses pass through the Jovian magnetosphere (Lanzerotti et al., 1992, 1993).

This field-aligned potential mechanism leads to local acceleration and thin auroral arcs. The loss cone instability mechanism, on the other hand, leads to diffuse auroras. Unfortunately, high spatial resolution measurements of shock auroras have not been analyzed to date, so the relative contributions of the two mechanisms cannot be assessed at the time.

8. Future Jupiter Studies

For the Earth's case, both plasma compression/field-aligned potential generation are viable mechanisms for shock-auroras. Ground-based observations are needed to determine the relative importance of each. For the Jovian auroral case, the loss-cone instabilities will be unimportant for the outer zone, but because of the strong compressibility of the (entire) magnetosphere, this mechanism may be important for the middle magnetospheric aurora oval as well. In the BL/outer zone region of Jupiter, field-aligned potential drops and discrete aurora would be expected from shock compression.

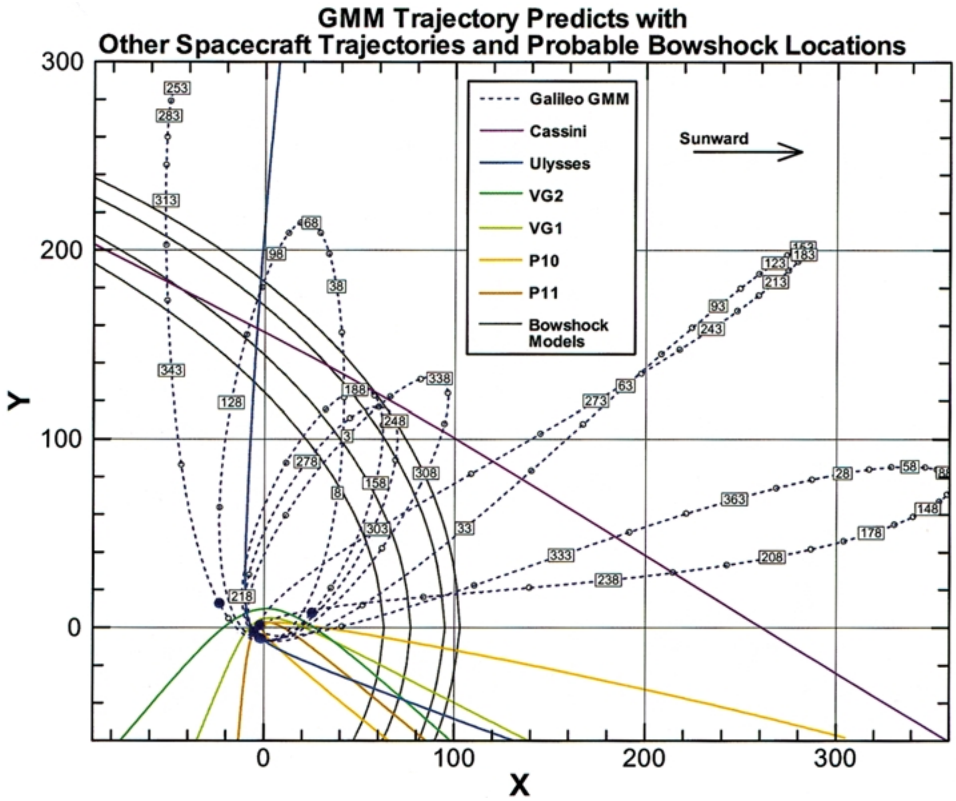

Figure 20. The Cassini flyby at Jupiter.

Shock compression of the magnetosphere and the consequential dayside aurora will help one 'map' the magnetopause magnetic field lines into the ionosphere. By obtaining the initial brightening and expansion of the dayside aurora, accurate magnetic field tracing can be obtained. Such a possibility at Jupiter will occur in October 2000 to March 2001 of this year. Cassini will make a flyby of Jupiter on its way to Saturn (Figure 20). Cassini will be constantly monitoring the solar wind field and plasma and detect interplanetary shock/pressure pulses near Jupiter. Cassini instrumentation will be able to image both the dayside and nightside auroral zones. The Galileo spacecraft which orbits Jupiter, will be inside the magnetosphere for part of this time and in interplanetary space for the other part. Magnetospheric compression effects, as well as auroral intensifications, will also be studied. Finally, HST will make dedicated Jovian auroral observations during selected intervals of this encounter period. Details of auroral intensifications, propagation and structure should be obtained from these searches.

9. Discovery of New Planets?

Finally, we would like to mention that the phenomenon of shock-auroras may be useful in the search for distant solar systems. In our solar system, strong optical flares at the sun are accompanied by fast plasma ejecta (CMEs) propagating into interplanetary space. These fast ejecta create the interplanetary shocks discussed here. If the shocks propagate toward and impinge up on a planetary magnetosphere, a shock aurora will be created. The spectra of the planetary aurora depends on the atmospheric constituents (and the energy of the precipitating charged particles) at the planet. Thus the auroral spectrum may be significantly different than that for the solar flare. What astronomers could look for are stars that have 'multiple flares' where the spectral characteristics vary consistently between the first, second, third, etc. flarings. The time between the flares would be related to the distances between the planets. If the shock speed could be estimated, these distances could be calculated.

Acknowledgments

Portions of this research was performed at the Jet Propulsion Laboratory, California Institute of Technology, under contract with the National Aeronautics and Space Administration. We wish to thank N. Krupp and R. Prangé for extending an invitation to present this paper at a European Geophysical Society meeting.

References

Akasofu, S.-I.: 1977, Physics of *Magnetospheric Substorms*, D. Reidel Publishing Co., Dordrecht, Holland.

Anderson, K.A., Lin, R.P., Paoli, R.J.,Parks, G.K. , Lin, C.S., Reme, H., Bosqued, J.M., Martel, F., Cotin, F. and Cros, A.: 1978, An experiment to study energetic particle fluxes in and beyond the Earth's outer magnetosphere, *IEEE Trans. Geosci. Elect. GE-16* 213.

Anderson, R.R., Harvey, C.C., Hoppe, M.M., Tsurutani, B.T., Eastman, T.E. and Etcheto, J.: 1982, Plasma waves near the magnetopause, *J. Geophys. Res.* **87**, 2087.

Axford, W.I. and Hines, C.O.: 1961, A unifying theory of high-latitude geophysical phenomena and geomagnetic storms, *Can. J. Phys.* **39**, 1433.

Bostrom, R., Gustafsson, G., Holback, B., Holmgren, G., Koskinen, H. and Kintner, P.: 1988, Characteristics of solitary waves and weak double layers in magnetospheric plasma, *Phys. Rev. Lett.* **61**, 82.

Carlson, C.W., Pfaff, R.F. and Watzin, J.G.: 1998, The Fast auroral snapshot (FAST) mission, *Geophys. Res. Lett.* **25**, 2013.

Chao, J.K. and Lepping, R.P.: 1974, A correlative study of ssc's, interplanetary shocks, and solar activity, *J. Geophys. Res.* **79**, 1799.

Chapman, S. and Ferraro, V.C.: 1931, A new theory of magnetic storms: Part I the initial phase, *Terr. Mag. Atmos. Elec.* **36**, 77.

Clark, J.T., Ballester, G., Trauger, J., Ajello, J., Pryor, W., Tobiska, K., Connerney, J.E.P., Gladstone, G.R., Waite, Jr., J.H., Jaffel, L.B. and Gérard, J.-C.: 1998, Hubble Space Telescope imaging of Jupiter's UV aurora during the Galileo orbiter mission, *J. Geophys. Res.* **103**, 20217.

Cowley, S.W.H.: 1995, Theoretical perspectives of the magnetopause: A tutorial review, *Phys. of the Magnetopause*, Am. Geophys. Un. Press, **90**, 29.

Dungey, J.W.: 1961, Interplanetary magnetic field and the auroral zones, *Phys. Rev. Lett.* **6**, 47.

Eastman, T.E., Greene, E.A., Christon, S.P., Gloeckler, G., Hamilton, D.C. and Ipavitch, F.M.: 1979. *Geophys. Res. Lett.* **17**, 7379.

Eastman, T.E.: 1979, The plasma boundary layer and magnetopause layer of the Earth's magnetosphere, LA-7842-T, LANL, New Mexico.

Elphic, R.C., Bonnell, J.W., Strangeway, R.J., Kepko, L., Ergun, R.E., McFadden, J.P., Carlson, C.W., Peria, W., Cattell, C.A., Klumpar, D., Shelley, E., Peterson, W., Moebius, E., Kistler, L. and Pfaff, R.: 1998, The auroral current circuit and field-aligned currents observed by FAST, *Geophys. Res. Lett.* **25**, 2033.

Ergun, R.E. et al.: 1998a, FAST satellite observations of large-amplitude solitary structures, *Geophys. Res. Lett.* **25**, 2041.

Ergun, R.E., Carlson, C.W., McFadden, J.P., Mozer, F.S., Muschietti, L. and Roth, I.: 1998b, Debye-scale plasma structures associated with magnetic field-aligned electric fields, *Phys. Rev. Lett.* **81**, 826.

Ergun, R.E., Carlson, C.W., Muschietti, L., Roth, I. and McFadden, J.P.: 1999, Properties of fast solitary structures, *Nonlinear Proc. Geophys.* **6**, 187.

Eviatar, A. and Wolf, R.A.: 1968, Transfer processes in the magnetopause, *J. Geophys. Res.* **73**, 5561.

Feldstein, Y.I. and Starkov, G.V.: 1970, The auroral oval and the boundary of closed field line of geomagnetic field, *Planet. Space Sci.* **18**, 501.

Goldman, M.V., Oppenheim, M.M. and Newman, D.L.: 1999a, Nonlinear two-stream instabilities as an explanation for auroral bipolar wave structures, *Geophys. Res. Lett.* **26**, 1821.

Goldman, M.V., Oppenheim, M.M. and Newman, D.L.: 1999b, Theory of localized bipolar wave structures and nonthermal particle distributions in the auroral ionosphere, *Nonlinear Proc. Geophys.* **6**, 221.

Gonzalez, W.D., Joselyn, J.A., Kamide, Y., Kroehl, H.W., Rostoker, G., Tsurutani, B.T. and Vasyliunas, V.M.: 1994, What is a geomagnetic storm?, *J. Geophys. Res.* **99**, 5771.

Grodent, D., Waite, Jr., J.H. and Gérard, J.-C.: 2000, A. self-consistent model of the Jovian auroral thermal structure, *J. Geophys. Res.*, submitted.

Gurnett, D.A. and Frank, L.A.: 1977, A region of intense plasma wave turbulence on auroral field lines, *J. Geophys. Res.* **82**, 1031.

Gurnett, D.A., Anderson, R.R., Tsurutani, B.T., Smith, E.J., Paschmann, G., Haerendel, G., Bame, S.J. and Russell, C.T.: 1979, Plasma wave turbulence at the magnetopause: Observations from ISEE1 and 2, *J. Geophys. Res.* **84**, 7043.

Haerendel, G.: 1994, Acceleration from field-aligned potential drops, *Astrophys. J. Suppl. Series* **90**, 765.

Intriligator, D.S. and Wolfe, J.H.: 1976, Results of the plasma analyzer experiment on Pioneers 10 and 11, in T. Gehrels (ed.), *Jupiter*, University of Arizona Press, 848.

Koskinen, H.E., Bostrom, J.R. and Holback, B.: 1987, Viking observations of solitary waves and weak double layers on auroral field lines, *Phys. of Space Plasmas* **7**, 147.

Lakhina, G.S., and Tsurutani, B.T.: 1999a, A generation mechanism for the polar cap boundary layer broadband plasma waves, *J. Geophys. Res.* **104**, 279.

Lakhina, G.S. and Tsurutani, B.T.: 1999b, Broadband plasma waves in the magnetopause and polar cap boundary layers, *Surveys in Geophys.* **20**, 377.

Lakhina, G.S., Tsurutani, B.T., Kojima, H. and Matsumoto, H.: 2000, 'Broadband' plasma waves in boundary layers, *J. Geophys. Res.* **105**, 27791.

Lanzerotti, L.J. et al.: 1993, Measurements of hot plasma in the magnetosphere of Jupiter, *Planet. Space Sci.* **41**, 893.

Lanzerotti, L.J., Armstrong, T.P., Gold, R.E., Anderson, K.A., Krimigis, S.M., Lin, R.P., Pick, M., Roelof, E.C., Sarris, E.T., Simnett, G.M., Maclennan, C.G., Chao, H.T. and Tappin, S.J.: 1992, The hot plasma environment at Jupiter: Ulysses results, *Science* **257**, 1518.

Lemaire, J.: 1977, Impulsive penetration of filamentary plasma elements into the magnetospheres of the Earth and Jupiter, *Planet. Space Sci.* **25**, 887.

Matsumoto, H., Kojima, H., Miyatake, T., Omura, Y., Okada, M., Nagano, I. and Tsutsui, M.: 1994, Electrostatic solitary waves (ESW) in the magnetotail: BEN waveforms observed by GEOTAIL, *Geophys. Res. Lett.* **21**, 2915.

Miura, A.: 1995, Kelvin-Helmholtz instability of the magnetopause: Computer simulations, *Phys. of the Magnetopause*, Am. Geophys. Un. Press, **90**, 285.

Muschietti, L., Roth, I., Ergun, R.E. and Carlson, C.W.: 1999, Analysis and simulation of BGK electron holes, *Nonlin. Proc. Geophys.* **6**, 211.

Omura, Y., Kojima, H. and Matsumoto, H.: 1994, Computer Simulation of electrostatic solitary waves: A nonlinear model of broadband electrostatic noise, *Geophys. Res. Lett.* **21**, 2923.

Omura, Y., Kojima, H., Miki, N., Mukai, T., Matsumoto, H. and Anderson, R.: 1999, Electrostatic solitary waves carried by diffused electron beams observed by the GEOTAIL spacecraft, *J. Geophys. Res.* **104**, 14627.

Parks, G.K., Lin, C.S., Anderson, K.A., Lin, R.P., Reme, H., Coroniti, F., Meng, C. and Pellat, R.: 1979, Particle boundary structures at the magnetopause and the plasmasheet, In *Magnetospheric Boundary Layers*, ESTEC, Noordwijk, Holland, 151.

Phillips, J.L., Bame, S.J., Thomsen, M.F., Goldstein, B.E. and Smith, E.J.: 1993, Ulysses plasma observations in the Jovian magnetosheath, *J. Geophys. Res.* **98**, 21189.

Prangé, R., Dougherty, N. and Dols, V.: 1993, Identification d'une aurorae, 'current-driven' sur Jupiter, 1(aide d(observations corréleés avec HST et Ulysses, In D. Hubert (ed.), *Compte-redus du Séminaire Scientifique du GdR Plasmas*, DESPA-Observatoire du Paris, 38.

Prangé, R., Maurice, S., Harris, W.M. and Livengood, T.: 1997, Comparison of IUE and HST diagnostic of the Jovian auroral morphology, *J. Geophys. Res.* **102**, 9289.

Reiff, P.H. and Hill, T.W.: 1979, Earth and Jupiter: Comparison of magnetopause structure, *Magnetospheric Boundary Layers*, ESA SP-148, 227.

Rezeau, L., Morane, A., Perraut, S., Roux, A. and Schmidt, R.: 1989, Characterization of Alfvénic fluctuations in the magnetopause boundary layer, *J. Geophys. Res.* **94**, 101.

Russell, C.T. and Elphic, R.C.: 1978, Initial ISEE magnetometer results: Magnetopause observations, *Space Sci. Rev.* **22**, 681.

Sonnerup, B.U.Ö., Smith, E.J., Tsurutani, B.T. and Wolfe, J.H.: 1981, Structure of Jupiter's magnetopause: Pioneer 10 and 11 observations, *J. Geophys. Res.* **86**, 3321.

Stone, R.G. et al.: 1992, The unified radio and plasma wave investigation, *Astron. Astrophys. Suppl. Series* **92**, 291.

Temerin, M., Cerny, K., Lottko, W. and Mozer, F.S.: 1982, Observations of double layers and solitary waves in the auroral plasma, *Phys. Rev. Lett.* **48**, 1175.

Treumann, R.A., LaBelle, J. and Bauer, T.M.: 1995, Diffusion processes: An observational perspective, In *Physics of the Magnetopause, Geophys. Mon. 90*, Amer. Geophys. Union, Wash. D.C., 331.

Tsurutani, B.T. and Meng, C.-I.: 1972, Interplanetary magnetic field variations and substorm activity, *J. Geophys. Res.* **77**, 2964.

Tsurutani, B.T., Smith, E.J., Thorne, R.M., Anderson, R.R., Gurnett, D.A., Parks, G.K., Lin, C.S. and Russell, C.T.: 1981, Wave-particle interactions at the magnetopause: Contributions to the dayside aurora, *Geophys. Res. Lett.* **8**, 183.

Tsurutani, B.T. and Thorne, R.M.: 1982, Diffusion processes in the magnetopause boundary layer, *Geophys. Res. Lett.* **9**, 1247.

Tsurutani, B.T., Brinca, A.L., Smith, E.J., Okida, R.T., Anderson, R.R. and Eastman, T.E.: 1989, A statistical study of ELF-VLF plasma waves at the magnetopause, *J. Geophys. Res.* **94**, 1270.

Tsurutani, B.T., Southwood, D.J., Smith and E.J., Balogh, A.: 1993, A survey of low frequency waves at Jupiter: The Ulysses encounter, *J. Geophys. Res.* **98**, 21203.

Tsurutani, B.T. and Gonzalez, W.D.: 1995, The efficiency of 'viscous interaction' between the solar wind and the magnetosphere during intense northward IMF events, *Geophys. Res. Lett.* **22**, 663.

Tsurutani, B.T., Gonzalez, W.D., Gonzalez, A.L.C., Tang, F., Arballo, J.K. and Okada, M.: 1995, Interplanetary origin of geomagnetic activity in the declining phase of the solar cycle, *J. Geophys. Res.* **100**, 21717.

Tsurutani, B.T. and Lakhina, G.S.: 1997, Some basic concepts of wave- particle interactions in collisionless plasmas, *Rev. of Geophys.* **35**, 491.

Tsurutani, B.T., Arballo, J.K., Goldstein, B.E., Ho, C.M., Lakhina, G.S., Smith, E.J., Cornilleau-Wehrlin, N., Prangé, R., Lin, N., Kellogg, P., Phillips, J.L., Balogh, A., Krupp, N. and Kane, M.: 1997, Plasma wave characteristics of the Jovian magnetopause boundary layer: Relationship to the Jovian aurora?, *J. Geophys. Res.* **102**, 4751.

Tsurutani, B.T., Lakhina, G.S., Ho, C.M., Arballo, J.K., Galvan, C., Boonsiriseth, A., Pickett, J.S., Gurnett, D.A., Peterson, W.K. and Thorne, R.M.: 1998a, Broadband plasma waves observed in the polar cap boundary layer: Polar, *J. Geophys. Res.* **103**, 17351.

Tsurutani, B.T., Arballo, J.K., Lakhina, G.S., Ho, C.M., Buti, B., Pickett, J.S. and Gurnett, D.A.: 1998b, Plasma waves in the dayside polar cap boundary layer: Bipolar and monopolar electric pulses and whistler mode waves, *Geophys. Res. Lett.* **25**, 4117.

Tsurutani, B.T., Arballo, J.K., Galvan, C., Zhang, L.D., Zhou, X,-Y., Lakhina, G.S., Hada, T., Gonzalez, W.D., Pickett, J.S. and Gurnett, D.A.: 2001a, Polar cap boundary layer waves: An auroral zone phenomenon, *J. Geophys. Res.*, in press.

Tsurutani, B.T., Zhou, X.-Y., Arballo, J.K., Gonzalez, W.D., Lakhina, G.S., Vasyliunas, V., Pickett, J.S., Araki, T., Yang, H., Rostoker, G., Hughes, T.J., Lepping, R.P. and Berdichevsky, D.: 2001b, Auroral zone precipitation during magnetic storm initial phases, *J. Atmosph. Sol.-Terr. Physics*, in press.

Zhou, X.-Y. and Tsurutani, B.T.: 1999, Rapid intensification and propagation of the dayside aurora: Large scale interplanetary pressure pulses (fast shocks), *Geophys. Res. Lett.* **26**, 1097.